01 Jan 2023

Distinct Element Analysis Of Various Structural Element Responses For Coal Rib Support Simulation

A. Kirmaci

D. Guner

K. Karadeniz

Taghi Sherizadeh
Missouri University of Science and Technology, sherizadeh@mst.edu

Recommended Citation

A. Kirmaci et al., "Distinct Element Analysis Of Various Structural Element Responses For Coal Rib Support Simulation," *57th US Rock Mechanics/Geomechanics Symposium*, American Rock Mechanics Associaton, Jan 2023.
The definitive version is available at https://doi.org/10.56952/ARMA-2023-0782

ARMA 23–0782

Distinct element analysis of various structural element responses for coal rib support simulation

Kirmaci, A., Guner, D., Karadeniz, K. and Sherizadeh, T.
Missouri University of Science and Technology, Rolla, MO, USA

This paper was prepared for presentation at the 57th US Rock Mechanics/Geomechanics Symposium held in Atlanta, Georgia, USA, 25-28 June 2023. This paper was selected for presentation at the symposium by an ARMA Technical Program Committee based on a technical and critical review of the paper by a minimum of two technical reviewers. The material, as presented, does not necessarily reflect any position of ARMA, its officers, or members. Electronic reproduction, distribution, or storage of any part of this paper for commercial purposes without the written consent of ARMA is prohibited. Permission to reproduce in print is restricted to an abstract of not more than 200 words; illustrations may not be copied. The abstract must contain conspicuous acknowledgement of where and by whom the paper was presented.

ABSTRACT: Understanding the bolt responses for the efficacy of bolt performance during coal rib support applications plays a key role in controlling the stability of underground coal mine openings. Conducting pull-out tests is imperative to gain a better understanding of these responses. Field conditions such as block volume and degree of cleating may significantly impact bolt performance. These field conditions can be efficiently implemented in numerical modeling approaches, and selecting a proper structural element type for these numerical studies is crucial. This study developed a pull-out test model and compared the performance of structural elements as support members in the coal rib model using 3DEC, a three-dimensional distinct element-based numerical modeling code. This study covered commonly utilized cable, pile, and hybrid structural elements in rib models with explicitly introduced face cleats. The bolt response of numerical models was calibrated with the field data showing the load-displacement response of a pull-out test. Comparing the rib models with these structural elements showed that hybrid structural elements demonstrated better agreement with the field observation as they can simulate the reaction to shearing along the discontinuities by inducing bending stresses. The impact of support density on rib stability is also presented in this study.

1. INTRODUCTION

The fact that injuries and fatalities linked to rib failure persist in underground coal mines, despite measures taken to ensure rib stability emphasizes the urgent need to develop and validate support systems that can effectively reduce coal rib failures. Currently, there is no standard practice for coal rib supports that can effectively address the diverse range of conditions encountered in coal mines across the United States (Guner et al., 2023). That leaves mine operators with no option but to rely on trial-and-error or industrial legacy practices. The severity of rib instabilities as a ground control hazard in underground coal mines is highlighted by the average annual fatality rate caused by coal rib failures, which remained at 1.6 between 2009 and 2022, as reported by MSHA (2022). Although coal rib failures pose a significant risk to the safety of the miners, there is limited information on these events and how rib support can mitigate them. Therefore, conducting studies to analyze the current rib support strategies and reduce injuries and fatalities resulting from rib failures in the coal mining industry is essential.

Numerical modeling approaches are widely used tools to understand the rib failure mechanisms and enhance the current body of knowledge to mitigate these rib-related risks. Through validated models, it brings the advantage of conducting parametric studies, including various coal types, overburden depth, mining height, and support systems. Numerical analyses, including pull-out test modeling and the effect of different support types on coal rib stability, can also enhance the design of coal rib supports.

Most of the authors' understanding of the rock-bolt interactions was supported by the load-displacement curves developed from pull-out testing simulations during numerical model efforts (Chen et al., 2018; Chen and Li, 2022; Saadat and Taheri, 2020). Bolt anchorage capacity and shear stiffness are the two main parameters that directly control the response of these support elements in coal ribs (Bastami et al., 2017). To better understand the coal rib-rock bolt interaction effect, a series of in-situ coal rib pull-out tests can be performed by recording the load and deformation. These field tests exhibit the load transfer mechanism between the bolt and the surrounding rock strata (Cox and Fuller, 1977; Schmuck, 1979; Jin-feng and Peng-hao, 2019). These tests are also significant for determining the bolt failure mechanisms, which can be seen as a combination of pull-out and shear stresses resulting in some of the jointed rock mass conditions during field applications (Li et al., 2016). In other words, understanding the rock bolt failure process in a jointed rock mass or cleated coal seam is essential because of the critical effects of the shear stresses (Chen and Li, 2015).

Commercially available numerical codes include various structural elements to simulate support systems. Currently, the most common structural element types

used in 3DEC to simulate the rib or roof bolts are the pile, cable, and hybrid structural elements (Itasca, 2022). Researchers widely use these structural elements: for instance, Mohamed et al. (2020) used the cable structural element, Chen and Li (2022), Rashed et al. (2019), and Tulu et al. (2012) assigned the pile elements for simulating the rock support response and Skarveles (2021) defined hybrid structural elements to simulate the rib bolts in their studies. The selection of structural element type depends mainly on application purpose and environmental conditions. This study compares the coal rib support models having cable, pile, and hybrid structural elements. The structural elements' parameters were obtained from the pull-out test simulation of the face-cleated coal rib models using the 3DEC.

2. STRUCTURAL ELEMENTS

Multiple structural elements in 3DEC numerical code can be used to simulate support systems. The application of structural elements may vary depending on the geological conditions and application requirements. Liner elements could be employed to simulate the bearing plates or other aerial support elements such as shotcrete, whereas the cable, pile, and hybrid structural elements can simulate rock and rib bolts.

2.1. Cable Structural Elements

Cable structural elements are suitable if bending forces are negligible since they offer shearing resistance due to the grout characteristics along their length. A reinforcement system's bonding agent (grout), which may fail in shear over a reinforcement section, can be modeled (such as cable bolts). Each cable element is characterized by geometric, material, and grout property assignments. A cable element has a straight length between two nodal locations with uniform cross-sectional and material properties. The cable element behaves as an elastic, perfectly plastic material that can yield in tension and compression but cannot resist a bending moment by the numeric code's default characteristics. Cable elements are good choices when simulating structural support systems with significant tensile capacity and axially oriented frictional contact with the rock or soil mass (Itasca, 2022).

2.2. Pile Structural Elements

Pile structural element is defined by geometric, material, and coupling-spring parameters. A straight segment with uniform, bi-symmetrical cross-sectional properties between two nodal points is considered a pile element. A curvilinear pile structure element can simulate a curved support element. Pile elements are appropriate for simulating structural-support parts like foundation piles, where frictional contact with the rock or soil mass occurs in both normal and shear directions (Itasca, 2022).

2.3. Hybrid Elements

Hybrid structural elements demonstrate similar responses with cable elements but include a dowel element (see Fig 1.) to prevent the cable from shearing perpendicular where it passes a joint or interface. The shearing of standard cable elements perpendicular to the cable part is not resistive. However, it is known that bolts crossing joints will offer some resistance to shearing on the joints when cables are used to represent bolts. In such cases, cable structural elements may be inefficient in simulating the rib bolt behavior, and hybrid structural elements may contribute to obtaining more accurate results. Skarveles (2021) used hybrid structural elements in 3DEC to evaluate the interaction between jointed rock and rock bolts and concluded that in cases where excessive shearing takes place due to fault movement, the hybrid element is the most promising alternative among all structural elements.

Dowel refers to various sophisticated mechanical actions, including the bending of steel bolts and the crushing of grout and the host rock. A shear spring that resists slipping on the fault where the bolt crosses simulate the dowel effect. In order to simulate the reinforcement effect, the dowel element needs additional parameters, such as active dowel length, dowel stiffness, yield force, and failure strain limit. These parameters were obtained using a calibration tool developed by Itasca (Itasca, 2022).

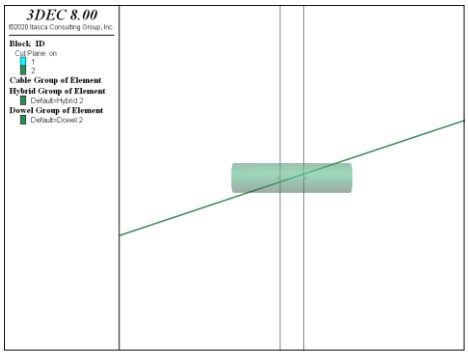

Fig.1. A hybrid structural element with a dowel element crossing a discontinuity at an angle (Itasca, 2022)

3. NUMERICAL MODELING AND THE CALIBRATION OF THE DATA

This study developed a pull-out test model and compared the performance of structural elements as a support member in the coal rib model using 3DEC, a three-dimensional distinct element-based numerical modeling code. Initially, the pull-out test model was calibrated using the dataset from Mohamed et al. (2020)'s study. The model with face cleats for a 1.2 m long mechanical bolt applied to the coal block is shown in Fig. 2. In this study, the coal-mass constitutive model, developed by Mohamed et al. (2018) to represents the loading and deformation process of the coal ribs accurately, was assigned to the model. This constitutive model was

developed by using coal samples' laboratory testing results and coal pillars' in-situ testing outcomes to obtain the equations related to the coal mass scales.

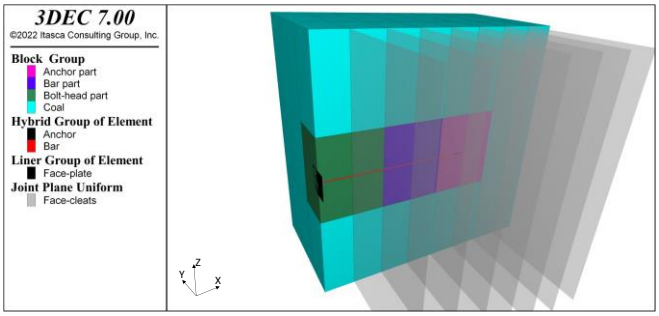

Fig. 2. The 3DEC coal model with face cleats for the application of mechanical bolt

According to the in-situ pull-out test results, the mechanical bolts showed a tri-linear load-displacement response. The mechanical bolt parameters used in the numerical models are listed in Table 1.

Table 1. Mechanical bolt parameters used in the models (Mohamed et al., 2020)

Parameter	Value
Bolt length (m)	1.2
Anchor length (m)	0.076
Free length (m)	1.124
Bolt diameter (mm)	16
Hole diameter (mm)	35
Steel Young's Modulus (GPa)	200
Yield load (kN)	102
Grout cohesion (kN/m)	823

Cable, pile, and hybrid structural elements were utilized in 3DEC to compare the efficacy of the structural elements for the different coal rib models. The cable structural element characteristics listed in Table 1., are consistent with the mechanical bolt parameters. Required moment of inertia values for pile elements was calculated as 3.11×10^{-9} m^4 considering the cross-sectional area characteristics of the support system. The dowel section needs additional parameters for hybrid structural elements, which are indicated in Table 2. These parameters were obtained using a calibration tool developed by Itasca.

The pull-out test of the mechanical bolts consists of the pre-tension and further loading process. Firstly, the bolts were pre-tensioned up to a point. 70% of the intercept of the second segment of the tri-linear load-displacement model was suggested to estimate the pre-tension load (Mohamed et al., 2020). Therefore, the mechanical bolts are initially subjected to a 24.5 kN axial force to simulate the pre-tension stage.

Table 2. The mechanical properties of dowel element used in the models

Parameter	Value
Dowel active length (m)	0.1
Dowel stiffness (MN/m)	10
Dowel yield force (kN)	11.2
Dowel failure strain limit	0.41

Three springs can be linked in series to simulate the interaction between coal and mechanical bolts. The first spring reflects the bar's stiffness. The second spring represents the interaction between the cone and shell leaves, and the third is the interaction between the shell leaves and coal. For ease of use, it was expected that the bearing plate would come into contact with coal without separation throughout the test and that there would be very little coal yielding at the bearing plate-coal contact zone. Therefore, it is possible to disregard the impact of the coal/bearing plate interaction.

The following steps were followed to obtain the anchor capacity and shear stiffness and calibrate the numerical model results with the experimental dataset, similar to the study conducted by Mohamed et al. (2020). Equations 1 - 5 were used to calculate these parameters. During the first section of the tri-linear load-displacement model (Fig. 3.), the coal at the anchoring point should remain undamaged, and the shell's leaves are entirely in contact with the coal. Except for the beginning of the second segment, the first section is insignificant to the mechanical bolt's anchoring mechanism. The bolt elongation and cone displacement are included in calculating the bolt head displacement in the first section. Therefore, the stiffness of the bar (K_b), see Eq.(1), and the stiffness of the cone/leaves contact (K_s) govern the slope of the first segment (K_{fs}) together as in Eq.(2):

$$K_b = \frac{E_b \times A_b}{L_b} \quad (1)$$

where E_b is Young's modulus of the steel, A_b is the cross-sectional area of the bolt, and L_b is the length of the bolt.

$$K_{fs} = \frac{K_b \times K_s}{K_b + K_s} \quad (2)$$

The coal at the anchoring point progressively yields in the second part of the tri-linear load-displacement model. Accordingly, the stiffness of the bolt (K_b), the cone/leaves contact (K_s), and the yielded coal (K_c) control the slope of the second segment (K_{ss}) as in Eq. (3):

$$K_{ss} = \frac{K_b \times K_s \times K_c}{K_b \times K_c + K_s \times K_b + K_s \times K_c} \quad (3)$$

The bolt reaches the anchorage capacity in the third part of the load-displacement plot, and the anchor starts to slip from the rib. It should be noted that coal strength and the bolt's geometry are the two main parameters to govern the anchorage capacity, and the anchorage capacity is independent of the magnitude of the installation torque.

The shear stiffness of the anchor differs in the first and second portions during the experiments. For the first portion, anchor stiffness was calculated (see Eq. (4)) with the stiffness of the cone/leaves contact (K_s) and anchored length (L_{anch}) by substituting Eq. (2).

$$Anchor\ stiffness_{fs} = \frac{K_{fs} \times K_b}{K_b - K_{fs}} \times \frac{1}{L_{anch}} \quad (4)$$

For the second portion, anchor stiffness was calculated (see Eq. (5)) with the stiffness of yielded coal (K_c) and anchor length (L_{anch}) by substituting Eq. (3).

$$Anchor\ stiffness_{ss} = \frac{K_b \times K_s \times K_{ss}}{K_s \times K_b - K_{ss} \times (K_s + K_b)} \times \frac{1}{L_{anch}} \quad (5)$$

By calculating the bolt parameters and properties in Eq. (4) and (5), the stiffness of the first and second portions was found as 171.3 and 30.1 MN/m^2, respectively. These calibrated values were used to design the structural elements applied to the coal rib model.

Fig. 3 represents the result of the in-situ pull-out test for the mechanical bolt and the load-displacement response obtained from the 3DEC numerical code. According to Fig. 3, the responses obtained by the 3DEC models match well with the in-situ pull-out test result.

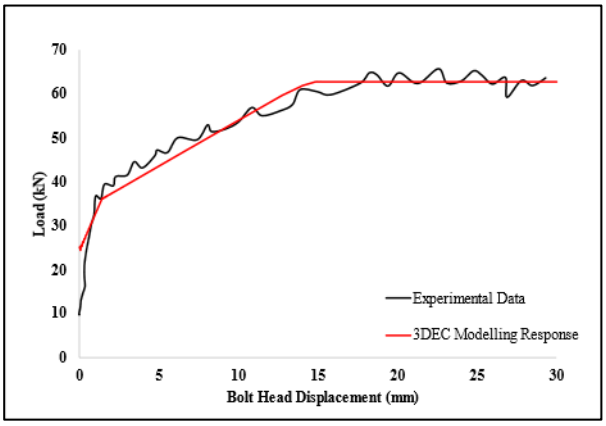

Fig.3. Load-displacement responses from the pull-out tests (Mohamed et al., 2020) and 3DEC numerical code.

Structural support elements were implemented using the coal rib models. A coal rib with a height of 3.3 m was simulated during the modeling process. The banded-bright coal with a laboratory uniaxial compressive strength value of 19.7 MPa, Young's modulus of 2.55 GPa, and Poisson's Ratio of 0.25 was assigned to the coal mass constitutive model. Further information about this constitutive model can be found in Mohamed et al. (2018). The roof and the floor strata were modeled using the elastic material model. Young's modulus and Poisson's ratio of the roof strata are taken as 8.3 GPa and 0.25, whereas 15.6 GPa and 0.25 for floor strata. The coal mass scale value of 20 was assigned according to the study of Rashed et al. (2019). They conducted the calibration process by iterating the coal-mass scale to satisfy visual observations and instrumentation results considering their field experiments. They obtained the best match when the coal mass scale was 20. The same coal type with the pull-out test models was selected to be consistent with the results. Face cleats were also introduced to the coal unit. The bottom of the model was fixed in the Z direction, while the sides were fixed in the X direction. The in-situ vertical stress was obtained by multiplying the coal density and the overburden depth. The roadway is assumed to be parallel to the maximum horizontal stress in the model, and the face cleats are also assigned in the same orientation, considering the most unfavorable case. The in-situ horizontal stresses in coal were calculated by the approaches presented by Liu et al. (2016). The following equations were used to calculate the maximum and minimum horizontal stresses on the coal seam:

$$\sigma_{Hc} = 1.174 + 0.024 \times Z_c \quad (6)$$

$$\sigma_{hc} = 0.018 \times Z_c - 1.475 \quad (7)$$

The in-situ horizontal stresses in the roof and floor rock units were calculated by the following equations (Esterhuizen, 2017, unpublished):

$$\sigma_{Hr} = 0.313 + 0.027 \times Z_r + 0.00278 \times E_r \quad (8)$$

$$\sigma_{hr} = 0.65 \times \sigma_{Hr} \quad (9)$$

Before excavating the roadway, the model was initially solved to achieve equilibrium under defined in-situ stress conditions. The reaction forces around the opening are stored, and the excavation boundaries are subjected to that force. The applied reaction force was nonlinearly reduced to simulate the more realistic ground reaction behavior along the opening. The rib bolts were activated when the rib face softened by 65%. Then, the model was solved to the final equilibrium following the installation of the rib bolts.

The one-bolted and two-bolted supported cases were first compared to a base-unsupported coal rib model that was constructed. The strength reduction factor (SRF) value is kept constant at 1 for these comparisons. Table 3 provides a list of the mechanical characteristics of coal mass.

Table 3. The mechanical properties of coal mass used in the coal rib model

Parameter	Value
Young's Modulus (GPa)	2.55
Poisson's Ratio	0.25
Laboratory UCS (MPa)	19.7
Coal-mass scale	20
Cleat spacing (cm)	25
Cleat Normal Stiffness, Kn (GPa/m)	100
Cleat Shear Stiffness Ks (GPa/m)	40
Cleat Peak Friction Angle	12
Cleat Res. Friction Angle	9
Cleat Peak Cohesion (MPa)	0.17
Cleat Resd. Cohesion (MPa)	0.06
Cleat Peak Tens Strength (MPa)	0.04
Cleat Resd. Tens Strength (MPa)	0.01

The model is built with a 3.3 m mining height and an overburden depth of 245 m. 1 cm displacement along a depth of 25 cm within the rib was used as the critical limit, which is considered as deformation-based criteria developed based on extensive field observations and numerical model outputs for the rib stability evaluation (Guner et al., 2022). The following numerical code outputs show the computation of the base models and observation of the effect of the application of support systems. The x-displacement plots for the unsupported scenario with an SRF value of 1 are presented in Fig. 4.

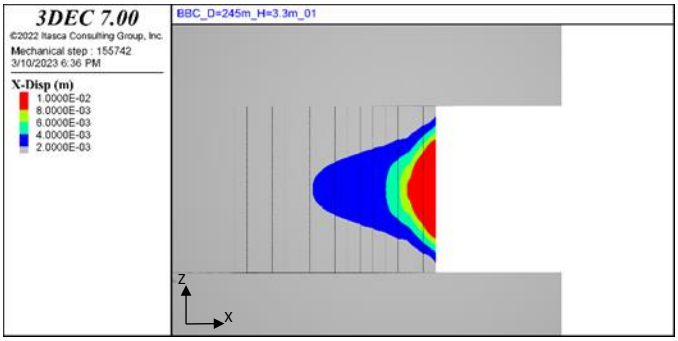

Fig.4. x-displacement contours obtained from the unsupported coal rib model (SRF=1)

The hybrid structural elements were first applied to the coal rib models to compare the results of unsupported and supported coal rib models. Fig. 5 indicates the x-displacement plots of the coal ribs supported with two identical hybrid structural elements.

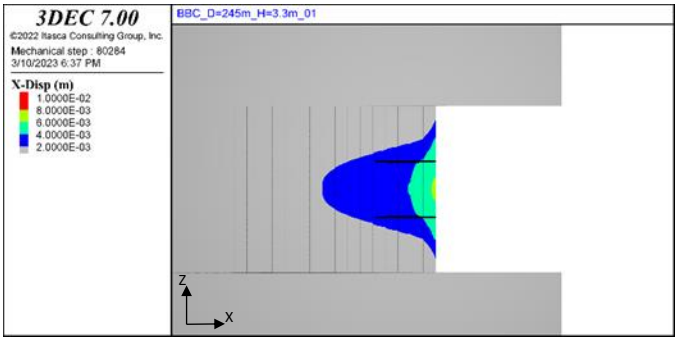

Fig.5. x-displacement contours obtained from the supported coal rib model with hybrid structural elements (SRF=1)

The displacement contours show a dramatic drop in comparison with the x-displacement findings of hybrid structural elements and unsupported models. While a 0.8 cm maximum displacement was observed in the rib's center in this case, the hybrid structural elements changed the rib's condition from unstable to stable.

Secondly, the cable elements were applied to the rib models. Fig. 6 indicates the x-displacement plots for the case and the rib deformation restriction impact of cable structural elements. The maximum rib deformations were observed to be slightly deeper into the rib because of the absence of the dowel segment in the cable structural element.

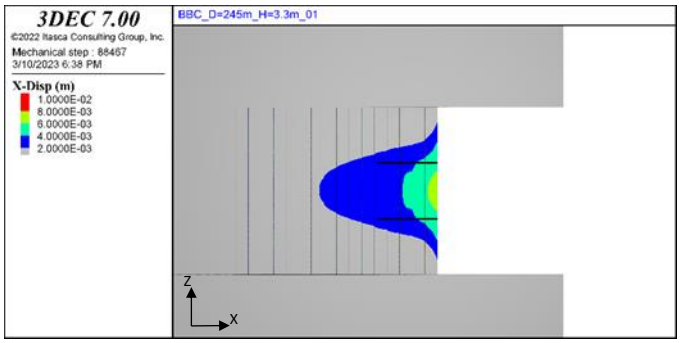

Fig.6. x-displacement contours obtained from the supported coal rib model with cable structural elements (SRF=1)

The pile structural elements were simulated considering the same mining case. The x-displacement plots on the coal rib with pile structural elements are shown in Fig. 7.

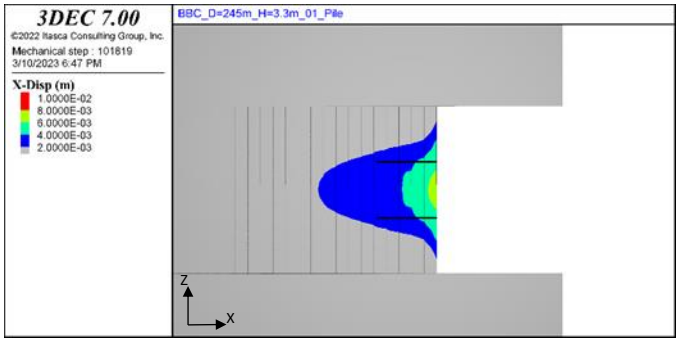

Fig.7. x-displacement contours obtained from the supported coal rib model with pile structural elements (SRF=1)

By taking into account the responses of x-displacement plots along the rib, the pile elements exhibited the same behavior as the cable elements.

The displacement profiles from the center point for each scenario were drawn to represent better the work done by each structural element (see Fig. 8). The performance of each structural element was analyzed by comparing the displacement profiles at the mid-height of the rib. The red point represents the critical limit for the rib stability evaluation on the plot. The curves below this point indicate the stable condition, whereas any curve above that point displays the unstable region.

Fig. 8 shows that the responses of the cable and pile structural elements were identical for the analyzed case as well as the x-displacement plot comparison. Additionally, the resistance of the bolt to axial forces locally can provide some resistance to the displacement caused by shear stresses along vertical discontinuities (Bouzeran et al., 2017), and it requires further investigation in future studies. It is noteworthy to mention that there is a possibility to observe different behaviors depending on the mining scenarios and the application type of the structural element. The work done by the hybrid structural elements is greater than the other structural elements due to the existence of the dowel segments.

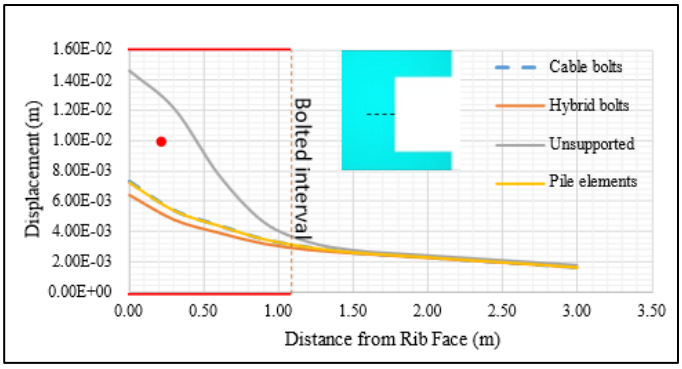

Fig.8. Displacement profiles for the unsupported and supported models with cable, pile, and hybrid elements

For the same mining scenario, the impact of support density was studied to better understand the effect of primary rib support density on rib stability as well. The hybrid structural element type was selected for the simulation of the bolts by considering the previous analysis of the structural element type. In this section, the SRF value was changed to 1.5 since most coal mines opt for rib support for RibFOS values less than 1.5 (Mohamed, 2021). The unsupported coal rib model's x-displacement values are shown in Fig. 9.

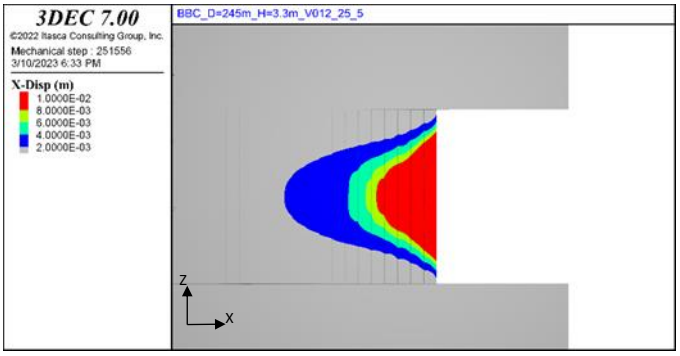

Fig.9. x-displacement contours obtained from the unsupported coal rib model (SRF=1.5)

Displacement contours in Fig. 9 show that more than 1 cm displacement on the rib can extend up to 1 m within the rib. The unsupported condition is therefore classified as unstable. Using the calibrated values acquired from the pull-out test models, a single hybrid structural element is installed as a primary support member at the mid-height of the rib. Fig. 10 illustrates the rib deformation response with a single bolt.

Installing a single bolt at the rib was observed to have a minimal impact on the coal rib stability. Considering the rib displacement plots, the decrease in critical rib deformation depth change, shown in red color in Fig. 9 and 10, is around 10 cm. Two bolted rib scenarios were also analyzed with a 1.1 m bolt spacing. The x displacement plots for this case is shown in Fig. 11.

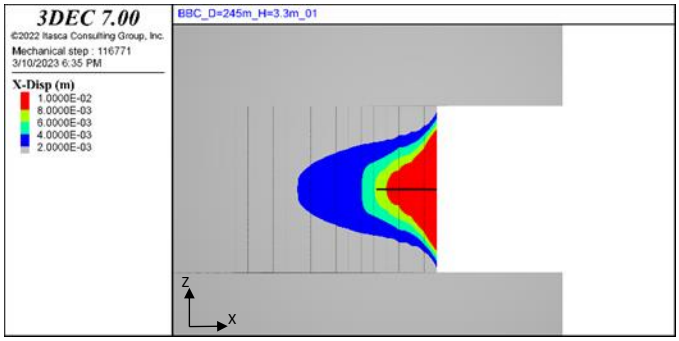

Fig.10. x-displacement contours obtained from the supported coal rib model with one bolt at the center of the rib (SRF=1.5)

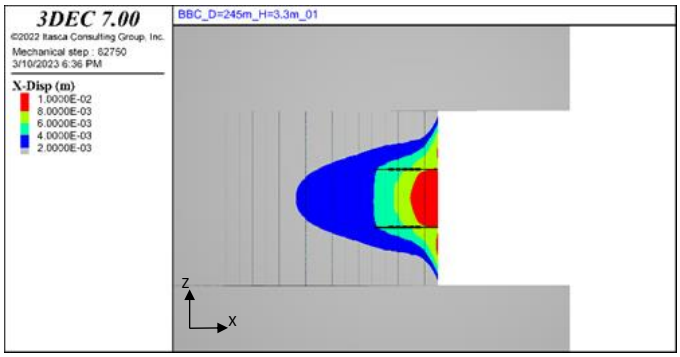

Fig.11. x-displacement contours obtained from the supported coal rib model with two bolts (SRF=1.5)

The coal rib supported by two identical bolts exhibits significantly restricted deformations. Compared to the outcomes of the unsupported and one-bolted cases, the depth of the rib deformation substantially decreased. Nevertheless, a 50 cm depth within the rib still indicates an unstable case at an SRF of 1.5. Displacement profiles were plotted at the rib's mid-height to understand the bolt application's impact better. The displacement at that profile line is shown in Fig. 12.

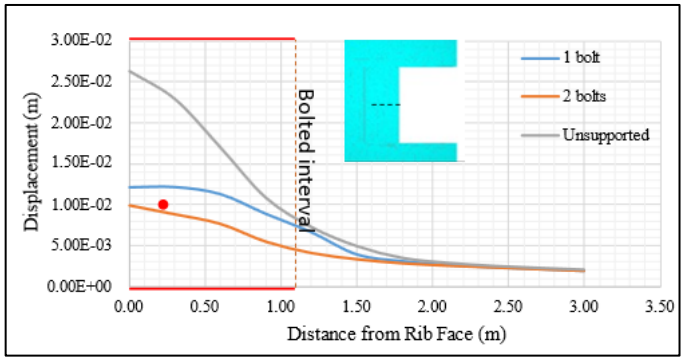

Fig.12. Displacement profile for the base models with unsupported, one-bolted, and two-bolted cases

4. CONCLUSIONS

The main focus of this study was to investigate rib-related failures by evaluating the effectiveness of various structural elements in enhancing rib stability through numerical simulation. The responses of the employed structural elements were calibrated using values obtained from field pull-out tests. The study utilized three types of

structural elements, namely cable elements, pile elements, and hybrid elements. The responses of these structural elements were examined under identical conditions. Based on the results obtained from the numerical techniques, the study yielded the following outcomes:

- The type of structural element will significantly impact the overall stability of the rib, depending on its geological conditions.
- Due to the application design and formulation of the pile and cable elements, they resulted in comparable responses when they were applied to the rib.
- Using hybrid structural elements to model the support system demonstrated a better rib bolt response for the jointed rock mass conditions.
- The work done by the hybrid structural elements is greater than the other structural elements due to the existence of the dowel segments. Therefore, it can be suggested that hybrid structural elements are preferable alternatives to bolts in jointed rock masses or cleated coal seams since they offer shearing resistance in jointed rock conditions.

ACKNOWLEDGEMENTS

This study is the part of the project that the Alpha Foundation sponsored for the Improvement of Mine Safety and Health, Inc. (Alpha Foundation). The views, opinions, and recommendations expressed herein are solely those of the authors and do not imply any endorsement by the Alpha Foundation, its directors, and staff.

REFERENCES

1. Bastami, M., Shahriar, K., and Ghadimi, M. (2017). Verification of the analytical model for fully grouted rock bolts based on pull-out test (case study: Tabas coal mine). In *ISRM European Rock Mechanics Symposium-EUROCK 2017*. OnePetro.
2. Bouzeran, L., Furtney, J., Pierce, M., Hazzard, J., and Lemos, J. V. (2017). Simulation of ground support performance in highly fractured and bulked rock masses with advanced 3DEC bolt model. *In Deep Mining 2017: Proceedings of the Eighth International Conference on Deep and High Stress Mining (pp. 667-680)*. Australian Centre for Geomechanics.
3. Chen, J., Saydam, S., and Hagan, P. C. (2018). Numerical simulation of the pull-out behaviour of fully grouted cable bolts. *Construction and Building Materials*, 191: 1148-1158.
4. Chen, J. and Li, D. (2022). Numerical simulation of fully encapsulated rock bolts with a tri-linear constitutive relation. *Tunnelling and Underground Space Technology*, 120, 104265.
5. Chen, Y. and Li, C. C. (2015). Performance of fully encapsulated rebar bolts and D-Bolts under combined pull-and-shear loading. *Tunnelling and Underground Space Technology*, 45, 99-106.
6. Cox, R. H., and Fuller, P. G. (1977). Load transfer behaviour between steel reinforcement and cement-based grout. *Division of Applied Geomechanics*, 1-12
7. Esterhuizen, G.S., 2017. Personal communication
8. Guner, D., Nowak, S., Sherizadeh, T., Sunkpal, M., Mohamed, K., and Xue, Y. (2023). Review of Current Coal Rib Control Practices. *Underground Space*, 9, 53-75.
9. Guner, D., Sherizadeh, T., Nowak, S., and Karadeniz, K.E. (2022). Distinct element analysis for the effectiveness of preliminary coal pillar rib support systems based on the strength reduction method. In *International Conference on Ground Control in Mining*, Canonsburg, PA. Society for Mining, Metallurgy and Exploration.
10. Itasca Consulting Group, Inc., (2022). 3DEC Ver. 7.0. Minneapolis, U.S.
11. Jin-feng, Z. and Peng-hao, Z. (2019). Analytical model of fully grouted bolts in pull-out tests and in situ rock masses. *International Journal of Rock Mechanics and Mining Sciences*, 113, 278-294.
12. Li, X., Aziz, N., Mirzaghorbanali, A. and Nemcik, J. (2016). Behavior of fiber glass bolts, rock bolts and cable bolts in shear. *Rock Mechanics and Rock Engineering*, 49, 2723-2735.
13. Liu, H., Sang, S., Xue, J., Wang, G., Xu, H., Ren, B., ... and Liu, S. (2016). Characteristics of an in situ stress field and its control on coal fractures and coal permeability in the Gucheng block, southern Qinshui Basin, China. *Journal of Natural Gas Science and Engineering*, 36, 1130-1139.
14. Mohamed, K., Rashed, G., Sears, M., Rusnak, J., and Van Dyke, M. (2018). Calibration of coal-mass model using in-situ coal pillar strength study. *SME annual conference and expo*, Minneapolis, MN.
15. Mohamed, K., Rashed, G. and Radakovic-Guzina, Z. (2020). Loading characteristics of mechanical rib bolts determined through testing and numerical modeling. *International journal of mining science and technology*, 30(1): 17-24.
16. Mohamed, K., Xue, Y., Rashed, G. and Kimutis, R. (2021). Analyzing Rib Stability and Support Using A Coal Pillar Rib Rating. In *International Conference on Ground Control in Mining*, Canonsburg, PA. Society for Mining, Metallurgy and Exploration.
17. MSHA. (2021). Fatality Reports, Mine Safety and Health Administration (MSHA). https://www.msha.gov/data-and-reports/fatality-reports/
18. Peng, S. S. and Tang, D. H. Y. (1984). Roof bolting in underground mining: a state-of-the-art review. *International Journal of Mining Engineering*, 2(1): 1-42.
19. Rashed, G., Sears, M., Addis, J., Mohamed, K. and Wickline, J. (2019). A case-study of roof support alternatives for deep cover room-and-pillar retreat mining using in-situ monitoring and numerical modeling. *Pre-print*, Minneapolis, Minnesota, USA: 25-28.
20. Saadat, M. and Taheri, A. (2020). Effect of contributing parameters on the behaviour of a bolted rock joint subjected to combined pull-and-shear loading: a DEM approach. *Rock Mechanics and Rock Engineering*, 53(1): 383-409.

21. Schmuck, C. H. (1979). Cable bolting at the Homestake gold mine. *Mining Engineering*, 31(12): 1677-1681.
22. Skarvelas, G. A. (2021). Reinforcement and Bonded Block Modelling. (Dissertation). Retrieved from http://urn.kb.se/resolve?urn=urn:nbn:se:ltu:diva-85984
23. Tulu, I. B., Esterhuizen, G. S. and Heasley, K. A. (2012). Calibration of FLAC3D to simulate the shear resistance of fully grouted rock bolts. In *46th US rock mechanics/geomechanics symposium. OnePetro*.